BRAIN
ORIGINAL ARTICLE

Stimulating native seizures with neural resonance: a new approach to localize the seizure onset zone

Rachel J. Smith,[1,2] Mark A. Hays,[1,3] Golnoosh Kamali,[2,4] Christopher Coogan,[3] Nathan E. Crone,[3] Joon Y. Kang[3] and Sridevi V. Sarma[1,2]

Successful outcomes in epilepsy surgery rely on the accurate localization of the seizure onset zone. Localizing the seizure onset zone is often a costly and time-consuming process wherein a patient undergoes intracranial EEG monitoring, and a team of clinicians wait for seizures to occur. Clinicians then analyse the intracranial EEG before each seizure onset to identify the seizure onset zone and localization accuracy increases when more seizures are captured. In this study, we develop a new approach to guide clinicians to actively elicit seizures with electrical stimulation. We propose that a brain region belongs to the seizure onset zone if a periodic stimulation at a particular frequency produces large amplitude oscillations in the intracranial EEG network that propagate seizure activity. Such responses occur when there is 'resonance' in the intracranial EEG network, and the resonant frequency can be detected by observing a sharp peak in the magnitude versus frequency response curve, called a Bode plot. To test our hypothesis, we analysed single-pulse electrical stimulation response data in 32 epilepsy patients undergoing intracranial EEG monitoring. For each patient and each stimulated brain region, we constructed a Bode plot by estimating a transfer function model from the intracranial EEG 'impulse' or single-pulse electrical stimulation response. The Bode plots were then analysed for evidence of resonance. First, we showed that when Bode plot features were used as a marker of the seizure onset zone, it distinguished successful from failed surgical outcomes with an area under the curve of 0.83, an accuracy that surpassed current methods of analysis with cortico-cortical evoked potential amplitude and cortico-cortical spectral responses. Then, we retrospectively showed that three out of five native seizures accidentally triggered in four patients during routine periodic stimulation at a given frequency corresponded to a resonant peak in the Bode plot. Last, we prospectively stimulated peak resonant frequencies gleaned from the Bode plots to elicit seizures in six patients, and this resulted in an induction of three seizures and three auras in these patients. These findings suggest neural resonance as a new biomarker of the seizure onset zone that can guide clinicians in eliciting native seizures to more quickly and accurately localize the seizure onset zone.

1 Department of Biomedical Engineering, Johns Hopkins University, Baltimore, MD 21218, USA
2 Institute for Computational Medicine, Johns Hopkins University, Baltimore, MD 21218, USA
3 Department of Neurology, Johns Hopkins University, Baltimore, MD 21287, USA
4 Department of Electrical and Computer Engineering, Johns Hopkins University, Baltimore, MD 21218, USA

Correspondence to: Rachel J. Smith
318 Hackerman Hall
3400 N. Charles St
Baltimore, MD 21218, USA
E-mail: rsmit249@jhu.edu

Keywords: dynamical network model; cortico-cortical evoked potentials; single-pulse electrical stimulation; seizure induction; surgical outcome

Received January 19, 2022. Revised May 02, 2022. Accepted May 26, 2022. Advance access publication June 15, 2022

Abbreviations: AUC = area under the curve; CCEP = cortico-cortical evoked potential; CCSR = cortico-cortical spectral responses; PW = peak-to-width; SIS = stimulation-induced seizures; SOZ = seizure onset zone; SPES = single-pulse electrical stimulation; TFM = transfer function model

Introduction

Epilepsy is a devastating disease with an estimated global lifetime prevalence of 100 million people worldwide.[1] First-line treatment for patients with epilepsy is anti-epileptic drugs, but ~30% of patients have persistent seizures despite a cocktail of these strong medications.[2] Surgical resection of the epileptogenic zone, the seizure onset zone (SOZ) and early spread regions can be an effective therapy for drug-resistant epilepsy patients,[3] but the lack of a clinically validated biomarker has made localizing the SOZ difficult and this prohibits widespread surgical success.[4–8]

Localizing the SOZ is a costly and time-consuming process during which a team of clinicians obtain imaging data (e.g. MRI, PET) and scalp EEG recordings, which is often followed by invasive monitoring involving days to weeks of EEG recordings captured intracranially (iEEG).[9] Clinicians visually inspect iEEG data, looking for abnormal activity (e.g. low-voltage, high-frequency activity, epileptiform discharges) on individual channels occurring immediately before seizures. Intracranial EEG offers a unique opportunity to observe rich epileptic cortical network dynamics, which are only visible by the naked eye during seizures. But, waiting for seizures to occur is risky for the patient as invasive monitoring is associated with complications including bleedings, infections and neurological deficits.[9] Further, the costs of monitoring are very high; it is estimated that the cost is at least US $5000 per day.[10,11]

There is emerging evidence that stimulation-induced seizures (SIS) may help identify the SOZ, especially when the semiology of the SIS is similar to the patient's native seizures.[12–14] Although periodic cortical stimulation is widely practised for functional mapping, the correlation between SIS and surgical outcome has been relatively understudied.[13] Because of this gap in knowledge, there are few methodological investigations and no standardized protocols to elicit SIS. Stimulation parameters typically vary between low (0.5–1 Hz) and high (50–60 Hz) frequency, with both monopolar and bipolar stimulations and highly variable stimulation currents and durations.[14] Additionally, the rates of SIS can be highly variable, ranging from <5 to >30% of stimulations inducing seizures.[14–16] A patient-specific, data-driven approach is needed to define stimulation locations and frequencies that increase the chances of eliciting native seizures for seizure onset localization purposes.

In this study, we propose a new SOZ biomarker, neural resonance, to address this need. We hypothesize that a brain region belongs to the SOZ if a periodic stimulation input at a particular frequency can produce large responses in the brain network, triggering epileptogenic activity. Such responses occur when there is a 'resonant frequency' of the iEEG network, and this frequency can be detected by observing a sharp peak followed by a large roll-off in the magnitude versus frequency response curve, called a Bode plot. This hypothesis is inspired by photo-sensitive epilepsy, in which specific periodic visual stimulation in space and time can trigger seizures.[17,18] Similarly, focal seizures are often evoked through periodic stimuli in audiogenic and reflexive epilepsies.[19,20]

We tested our neural resonance hypothesis in 32 epilepsy patients undergoing iEEG monitoring. Single-pulse electrical stimulation (SPES) was performed in each patient by administering brief pulses of electrical current at various brain regions, including those annotated to be within and outside of the SOZ. For each patient and each stimulated brain region, we constructed a Bode plot by estimating a TFM from the SPES response. SPES responses presented an opportunity to investigate 'impulse responses' of the iEEG network. From the impulse responses, one can evaluate properties of the iEEG network with dynamical systems analysis via TFMs and Bode plots, including whether or not pathological resonance exists when stimulating specific brain regions. We first demonstrated that the SOZ displays pathologically high levels of resonance by correlating Bode plot features to surgical outcome. We then retrospectively identified resonant properties in brain regions that stimulated seizures during functional mapping or during the SPES procedure. Last, we showed that prospectively stimulating at the resonant frequency increases the likelihood of eliciting the patient's native seizure.

Materials and methods

Patients

In total, we included 32 patients who underwent intracranial monitoring and SPES before surgery for treatment of drug-resistant epilepsy from January 2016 to June 2021. The study was approved by the Johns Hopkins School of Medicine Institutional Review Board (IRB 00247294) and was conducted using guidelines established in accordance with the Code of Ethics of the World Medical Association (1964, Declaration of Helsinki). Twenty-eight of the 32 patients had surgery performed and were evaluated for surgical outcome, and these patients were analysed in the Retrospective Development section to correlate Bode plot features with outcome measures (Table 1). In 5 of the 32 patients, seizures were stimulated during the normal SPES procedure ($n = 1$) or during functional mapping at 50 Hz stimulation frequency ($n = 4$); these patients are included in the Retrospective Validation section (Table 2, top). In the Prospective Validation section, we prospectively stimulated 6 of the 32 patients ($n = 3$ with surgical outcome data) to elicit seizures. These patients were admitted to the JHH EMU between January and June 2021 (Table 2, bottom).

The SOZ, early propagation regions and irritative zone were determined by board-certified epileptologists, on the basis of a comprehensive evaluation of clinical demographic data, intracranial and scalp EEG, and non-invasive imaging. Channel annotations were assigned independently of the research study.

We used the Engel Outcome Scale to classify outcome after surgical treatment at least 6 months after the surgery date (19 of 32 were evaluated over 1 year since surgery). We defined successful surgical outcomes as Engel I or II (either seizure-free or few disabling seizures), and failure outcomes as Engel III or IV (seizure persistence or increase after surgery). Patients that achieved an Engel III score after implantation of a responsive neurostimulation system (RNS) were considered a surgical success because the therapy was indicated as palliative.

Table 1 Summary of clinical data for patients used in retrospective development

Patient number	Gender	Age	MRI	Electrode type	Stimulated sites/% SOZ	Outcome
P001	Female	43	Previous right anterior temporal lobectomy with amygdalohippocampectomy	Subdural electrodes	11/27%	Engel I
P002	Male	25	Non-lesional	Subdural electrodes	7/43%	Engel IV
P003	Female	43	Non-lesional	Subdural electrodes	8/37%	Engel IIIA
P004	Female	35	Left temporal DNET	Subdural electrodes	5/20%	Engel II
P005	Female	19	Right middle frontal gyrus dysplasia	Strip/Grid/Depth	11/27%	Engel I
P006	Male	32	Previous resections of left postcentral gyrus	Subdural electrodes	26/30%	Engel IV
P007	Female	26	Left periventricular heterotopia	SEEG	22/0%	Engel IV
P008	Male	49	Left mesial temporal sclerosis	Subdural electrodes	36/19%	Engel I
P009	Male	62	Multifocal encephalomalacia in the bilateral frontal lobes and in the left occipital lobe	SEEG	10/40%	Engel II
P010	Male	26	Non-lesional	Subdural electrodes	7/29%	Engel I
P011	Female	32	Previous left frontal resection	SEEG	26/12%	Engel IV
P012	Female	27	Bilateral occipital lissencephaly	SEEG	13/62%	Engel III: RNS, labelled as success
P013	Female	24	Previous left temporal resection	SEEG	9/22%	Engel I
P014	Female	26	Left frontal periventricular nodules	SEEG	19/21%	Engel II
P015	Female	51	Right mesial temporal sclerosis	SEEG	7/29%	Engel I
P016	Male	48	Periventricular bilateral nodular heterotopia and diffuse cortical dysgenesis	SEEG	17/12%	Engel I
P017	Female	23	Left temporal encephalomalacia	SEEG	18/28%	Engel III: RNS, labelled as success
P018	Male	32	Right parietal encephalomalacia	SEEG	14/36%	Engel I
P019	Female	35	Right mesial temporal sclerosis	SEEG	18/17%	Engel I
P020	Male	58	Non-lesional	SEEG	16/13%	Engel I
P021	Male	33	Right medial parietal lobe cystic lesion	SEEG	30/33%	Engel III
P022	Female	53	Right mesial archnoid cyst	SEEG	21/19%	Engel II
P023	Male	45	Prominent left amygdala and loss of internal architecture left hippocampus	SEEG	24/21%	Engel III
P024	Female	40	Prior left frontal resection	SEEG	39/28%	Engel I
P025	Male	21	Previous left hippocampal LiTT	Strip/Grid/Depth	46/2%	Engel I
P026	Female	48	Focal left fronto-parietal operculum dysplasia	SEEG	19/6%	Engel I
P027	Male	33	Non-lesional	SEEG	22/27%	Engel III
P028	Male	24	Non-lesional	SEEG	31/32%	Engel I

RNS = responsive neurostimulation system.

Electrode placement

Patients were implanted with stereoEEG (SEEG) electrodes or electrocorticography (ECoG) arrays. The electrodes were placed according to the suspected location of the epileptogenic zone in each patient, as determined by non-invasive tests including clinical seizure history, neuroimaging, neuropsychology and scalp EEG recordings. The macroelectrodes were 2.3 mm in diameter with 1 cm spacing (Adtech or PMT Corp.). The SEEG depths (AdTech Medical Instruments Corp.) were multi-contact, and consisted of 6 ± 10 cylindrical, 2.3 mm platinum contacts separated by 5 mm between centres of adjacent electrodes. SEEG electrodes were implanted stereotactically using the ROSA robotic assistant device (Medtech) as part of standard patient care. Using BioImage Suite [Xenophon Papademetris (2020) BioImage Suite Web], electrode locations were obtained for 18 of the 32 patients by coregistering the post-implantation CT and brain MRI. FreeSurfer parcellation and visual verification with post-implant MRI was used to identify electrodes within cortical and subcortical grey matter.

SPES data acquisition and preprocessing

A NeuroPort amplifier (Blackrock Microsystems) was used to record ECoG and SEEG data during SPES. These data were filtered (analogue Butterworth antialiasing filters: first-order high-pass at 0.3 Hz, third-order low-pass at 7500 Hz), digitized at 16-bit resolution and down-sampled to 1 kHz with a digital antialiasing filter. SPES was conducted using a CereStim R96 (Blackrock Microsystems). Stimulation was applied at 0.5 Hz frequency in a pseudo-bipolar manner to pairs of adjacent electrodes using square biphasic pulses (0.15 ms/phase) (Fig. 1A). Stimulation sites were chosen primarily in grey matter in patients recorded before 2020, but later expanded to include both grey and white matter sites. At each stimulation site, we recorded responses from 40–50 stimulation trials. The maximum current intensity used varied from 4 to 10 mA, and was determined by visual confirmation of consistent evoked potentials during real-time visualization by a board-certified neurologist.

SPES-derived transfer function model calculation

The average evoked response was measured for every iEEG contact in 2-s epochs beginning 6 ms before stimulus onset (Fig. 1B). Artefactual channels were removed from the dataset and electrical stimulation artefact was removed by replacing the data 4 ms before and 8 ms after stimulus onset with a linearly spaced vector between those voltage values. To identify artefactual channels, we time locked the responses to the time of stimulation and calculated the

Table 2 Stimulation parameters and clinical data for retrospective and prospective validation

Patient number	Symptomatic contacts	Frequency of stimulation	Native seizure/aura?	Clinical outcome	Bode match?
Retrospective Validation					
P001	*RPTS49-57*[a]	0.3 Hz	Yes	Engel I	Yes
P003	**BTG3-4**[a]	50 Hz	Yes	Engel IIIA	Yes
P011	**SENM1-2**[a]	50 Hz	Yes	Engel IV	Yes
P025	LFT45-46[a]	50 Hz	No	Engel I	No
P029	*LNB 1-2*[a], *LNC1-2*[a], RN1-2[c], **RN3-4**[c]	All 50 Hz	Yes	No surgery	No
Patient number	**Symptomatic contacts**	**Frequency of stimulation**	**Native seizure/aura?**	**Number of pairs tested**	**TPR/FPR/FNR**
Prospective validation					
P024	**ALL3-4**[b], LSM1-2[b]	15 Hz	Yes	9	TPR = 2/9 FPR = 7/9 FNR = 0/9
P027	**RHG2-3**[b]	20 Hz	Yes	8	TPR = 0/8 FPR = 7/8 FNR = 1/8
P028	**RAH1-2**[a], **LPH1-2**[b]	20 Hz, 18 Hz	Yes	2	TPR = 2/2 FPR = 0/2 FNR = 0/2
P030	INF9-10[a]	20 Hz	Unknown	10	TPR = 0/10 FPR = 9/10 FNR = 1/10
P031	*RAH1-2*[a], *RPH1-2*[c], **RTP1-2**[a]	13 and 15 Hz, 16 Hz, 1 Hz	Yes	10	TPR = 2/10 FPR = 7/10 FNR = 1/10
P032*	*LPBT1-2*[c], *LPH1-2*[c], **LAH1-2**[a]	33 Hz, 20 Hz, 33 Hz	Yes	13	TPR = 3/13 FPR = 10/13 FNR = 0/13

SOZ contacts are highlighted in bold; early propagation contacts are highlighted in italics. Non-SOZ contacts are in roman font. FPR = false positive rate; FNR = false negative rate; TPR = true positive rate.
[a]Stimulated seizure.
[b]Stimulated aura.
[c]Stimulated after-discharges.

standard deviation of trial values at each time point. We removed channels in which the median standard deviation value exceeded 800 μV, indicating the presence of large noise fluctuations in the data. Additionally, if the mean of the response waveform in 1800–2000 ms poststimulus was not within 200 μV of the mean of the prestimulus baseline (−500 to −10 ms), we assumed that the neuronal network was not back to resting state before the next trial. We excluded these channels to avoid introducing instabilities in the models. We also removed the stimulation channels from the models.

We additionally sought to remove non-responsive channels from the TFM. To do this, we swept through a range of parameters to find optimal channels to include. We first searched for the maximum amplitude difference in 30, 100, 200 and 300 ms after stimulus from the average prestimulus baseline value (−500 to −10 ms). We also swept through specific percentages of channels from which the highest amplitude responses were to be included in the model: 25, 50, 75 and 100% of response channels. From this parameter sweep, there were 16 total models we tested. We found that the model that best separated surgical outcome looked for responses in the first 100 ms after stimulation and included the top 50% of channels with the highest amplitude responses (Supplementary Fig. 1A). This subset of channels was used to build the TFM. Non-responsive channels were removed while blinded to clinical labelling of electrodes. Similar percentages of SOZ, early propagation and irritative zone electrodes were removed for each patient and across all patients (Supplementary Fig. 1B and C).

TFMs were constructed for each subject and each stimulating electrode contact pair to estimate the behaviour of the SPES evoked response (Fig. 1C). We built a stable, discrete, linear time invariant vector of TFMs for each stimulating contact of the following form:

$$\boldsymbol{H}(e^{-i\omega}) = \boldsymbol{C}(e^{-i\omega}I - \boldsymbol{A})^{-1}\boldsymbol{B} \quad (1)$$

where ω is frequency in radians, A, B and C are estimated via least-squares estimation as in Li *et al.*[21] Briefly, $A \in \mathbb{R}^{n\times n}$ is the state transition matrix, $B \in \mathbb{R}^{n\times 1}$ describes how the input signal influences the neural state vector, $\mathbf{C} \in \mathbb{R}^{n\times 1}$ is the matrix that scales the state vector to the output vector and n is the number of channels. The pair of stimulation electrodes was not included in the TFMs as variables and was instead characterized as providing an exogeneous input.

This resulted in a vector of transfer functions for one electrode stimulation pair $H_i(e^{-j\omega})$ where H_i denotes the vector of transfer functions from the input signal to all significant response signals for stimulation pair i. These TFMs represented the input–output behaviour of evoked responses under SPES, from which the magnitude was computed by the norm of the vector $H_i(e^{-i\omega})$ versus stimulation frequency (ω) plot.

Bode plot and peak-to-width ratio measurements

To quantify the resonant nature of the Bode plot, we computed the peak gain, as computed by the 2-norm of the model $H_i(e^{-i\omega})$ over all frequencies (ω). We denoted the peak gain, the local maxima with the largest magnitude, to be a_{max} and the peak frequency to be ω^*

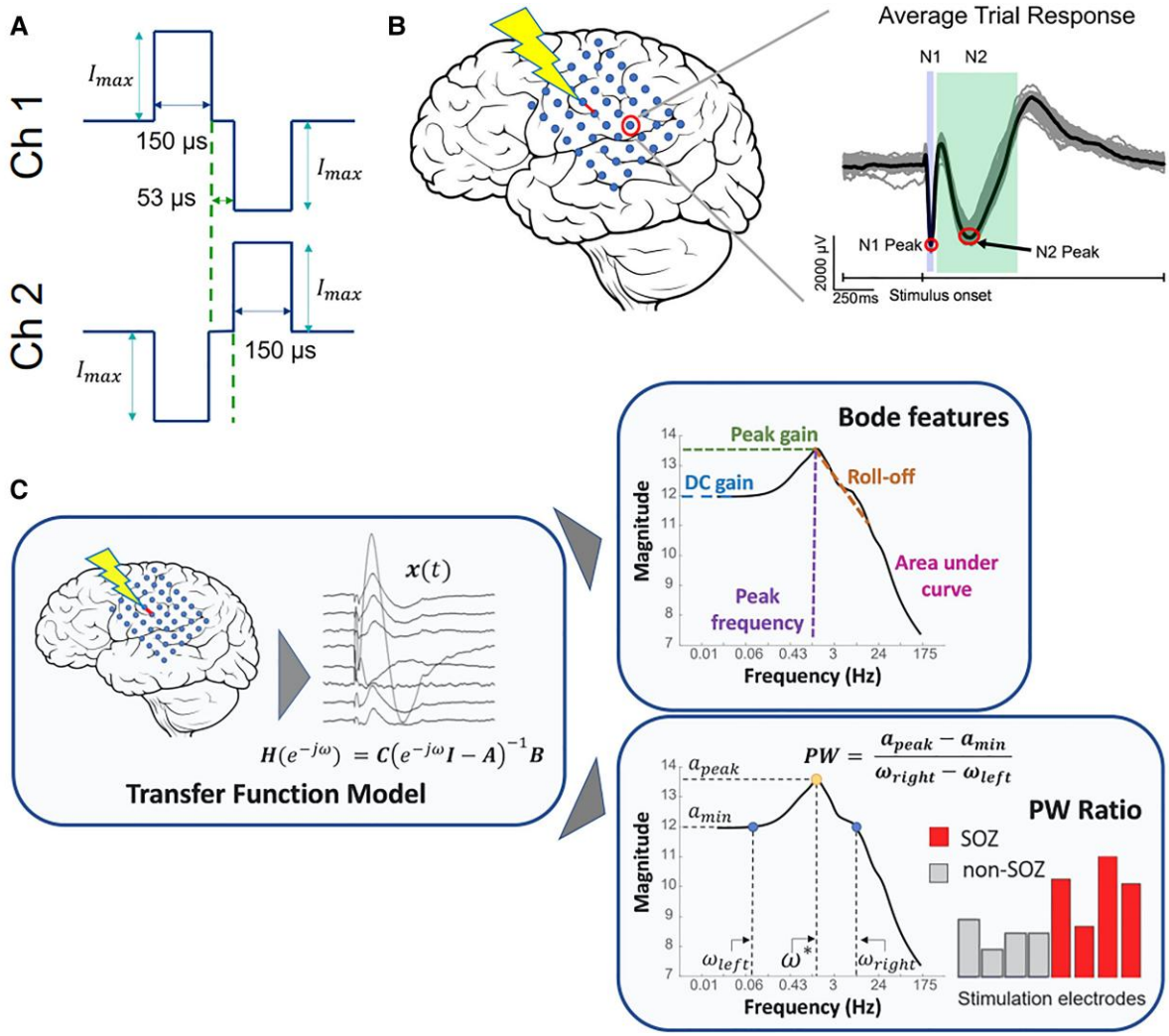

Figure 1 SPES evoked potential and pipeline to obtain Bode plots and PW ratios. (**A**) Stimulation applied in a pseudo-bipolar manner between two adjacent channels. (**B**) Stimulation elicits a response in remote electrodes. The typical waveform has a sharp negative peak 10–50 ms after the stimulus (N1) and a longer, lower amplitude peak 50–300 ms after the stimulus (N2). (**C**) In the *left* panel, a brain region is stimulated. The responses are captured and used to construct a TFM from the input signal. Next, we construct the Bode plot for the system, identify the resonant peaks and calculate the pertinent features (including PW ratio) from the function $PW = (a_{peak} - a_{min})/(\omega_{right} - \omega_{left})$.

(Fig. 1C). Note that we used ω^* as the stimulation frequency to elicit seizures (see Seizure Stimulation: Retrospective and Prospective Validation). To quantify the height of the peak in comparison to the surrounding gains on the log–log Bode plot, we calculated the gain value of the local minimum to the left (lower frequency) of the peak gain (named a_{min}), as well as its frequency correlate (ω_{left}). From that minimum, the gain value on the right side of the peak (higher frequency) that was closest to a_{min} was named the corresponding frequency (ω_{right}). The peak-to-width (PW) ratio was defined as the difference of the gains over the difference of the frequencies:

$$PW\ ratio = \frac{a_{max} - a_{min}}{\omega_{right} - \omega_{left}} \quad (2)$$

Thus, the PW ratio was maximized with large amplitude differences and small frequency differences, which would occur with prominent peaks in the Bode plot. We measured other pertinent features of the Bode plot, such as the DC gain, the roll-off and the area under the Bode curve. Additionally, because the dynamics of our TFMs resemble those of coupled mass-spring-damper systems, we are often able to identify multiple resonant peaks.[22] In some cases, we used secondary peaks for seizure stimulation because the peaks were sharper or in higher frequency ranges.

Model robustness testing

To ensure the TFMs accurately captured the iEEG responses, we compared the iEEG data to simulated data that were reconstructed from the model. First, we calculated the mean and standard deviation of the SPES stimulation trials in every recording electrode. We then reconstructed the average evoked waveform in each channel using a 2 ms pulse input and initial condition $x(0) = 0$. We calculated the fraction of the model-reconstructed data points that lay within 1 SD of the mean. We recorded the mean concordance of the reconstructed responses for each stimulation pair and reported the distributions of the mean concordances for each patient.

Additionally, we compared experimentally measured gains, which were derived from recorded iEEG data during stimulation,

to the gains represented by the Bode plots. There were three patients in which we performed repeated stimulation in one or two specific electrode pairs at varying frequencies. We first constructed the Bode plot for that stimulation pair from the TFM. Next, we experimentally determined the gain by computing the Frobenius norm of the iEEG responses divided by the norm of the input signal, which we defined as a square pulse 2 ms in duration with unit amplitude at the stimulation frequency. The experimentally derived gains were compared with the model-derived gains to assess model accuracy across varying frequencies.

Correlation of Bode plot features to surgical outcome: retrospective development

We implemented a threshold-based classifier on Bode plot metrics to investigate whether they correlated to surgical outcome. We calculated the difference between the Bode plot features [DC gain, the peak gain (H_∞) norm, the peak frequency (ω^*), the roll-off, the area under the Bode curve (area) and the PW ratio] for epileptogenic (SOZ, early propagation and irritative zone) contacts and non-epileptogenic contacts. The difference values were included as features in a logistic regression model. We hypothesized the patient was more likely to have a successful outcome when the difference in the features of epileptogenic and non-epileptogenic regions was large.

We also categorized surgical outcomes using both the cortico-cortical evoked potential (CCEP) amplitudes (N1 and N2), as defined by the z-score of the peak amplitude relative to the prestimulus baseline data, and cortico-cortical spectral responses (CCSRs), as defined by the mean power in centre frequencies of the canonical frequency bands across the epoch after the stimulus.

The N1 peak is an early negative deflection thought to represent the strength of the direct effective connectivity[23] and is a measure commonly used in SPES analysis to assess epileptogenicity.[24–26] For each stimulation pair in each patient, we calculated the mean z-score value for included channels. In a similar parameter sweep to test which channels to include, we tested four situations: including channels with z-scores in the top 25%, the top 50%, the top 75% and all channels. We found that surgical outcome was best separated when the top 25% of z-scores were included in the logistic regression model (Supplementary Fig. 2). We then tested whether the classification accuracy of our algorithm matched the CCEP amplitude metrics via comparison of the area under the curve (AUC) of each classifier and the distribution of probability values for each metric.

The spectral response to SPES has also recently been used to identify epileptogenic brain tissue.[27] To obtain the CCSRs, we adapted methods from Mitsuhashi *et al.*[28] First, we constructed Morlet wavelets according to the centre frequencies of the canonical frequency bands [theta (5–7 Hz) = 6 Hz; alpha (8–12 Hz) = 10 Hz; beta (14–30 Hz) = 22 Hz; gamma (31–60 Hz) = 45 Hz and high gamma (61–100 Hz) = 80 Hz].[29] The wavelets were each constructed with four cycles and were convolved over the entire trial window (2-s epoch) in 1 ms steps.[28] We removed stimulation artefact by replacing the data 4 ms before and 8 ms after stimulus onset with a linearly spaced vector between those voltage values. We computed the wavelet time-frequency decomposition for each trial and then averaged across all trials for the given stimulation pair. To obtain a single CCSR amplitude value in each frequency band per stimulation pair, we computed the mean across the trial time and recorded the square root of the averaged power.[28] In a similar way to the Bode metrics, we constructed features from the CCSR values by computing the difference between CCSRs in epileptogenic (SOZ, early propagation and irritative zone) regions and non-epileptogenic regions. We permuted all possible combinations of three of the five frequency bands to find which set gave the highest accuracy in predicting surgical outcome and compared this to the model with Bode features.

Seizure stimulation: retrospective and prospective validation

In five patients, seizures were elicited during cortical stimulation mapping or during the SPES procedure. In these patients, we retrospectively gathered SPES data from the sites that produced a SIS if it was available. With the SPES data, we built TFMs and analysed the Bode plots for resonant peaks at the frequency that stimulated the seizure.

In six patients, we prospectively tested whether our TFM could predict which brain regions and at what frequencies to stimulate to trigger a seizure or epileptiform activity. These patients underwent the SPES procedure, TFMs were built using the evoked responses immediately after the stimulation session concluded and Bode plots were created for each stimulation pair. Once the Bode plots were created, the most resonant nodes (nodes with the highest PW ratios and/or sharp secondary peaks) were identified and the peak frequency, ω^*, was recorded. A stimulation plan was developed for the clinicians to attempt to induce epileptiform activity, with nodes outside the suspected SOZ to be tested first and suspected SOZ nodes to be tested last. Stimulation was then administered in a bipolar manner to the resonant node pair using square biphasic pulses (0.15 ms/phase) at frequency ω^* for a duration of 3–5 s.[30] The iEEG recordings were visually inspected for epileptiform discharges, high-frequency activity or seizure activity. If it was observed that a seizure was not induced, the next stimulation pair was tested after a 30-s rest period. If a full seizure occurred, the stimulation procedure was terminated. If the seizure was successfully aborted by the clinical team, the stimulation procedure continued.

We defined the condition as the absence or presence of a stimulated seizure, and test as the output of the Bode plot (negative or positive). Therefore, a true positive test result was one which the research team told the clinical team to stimulate at ω^* and a seizure or aura was elicited. A false positive test result was one that the research team told the clinical team to stimulate ω^*, but no seizure or aura was elicited. In several cases, if a seizure was not elicited from the TFM predictions, the clinical team would stimulate for seizures on the basis of their clinical expertise. A false negative test result was defined as stimulations in which the clinical team elicited a seizure or aura when that stimulation parameter set was not predicted by the research team. Because of the longevity of the experiments and the rarity of SIS events, we did not stimulate regions that did not have a resonant peak; thus, true negatives were not fully assessed. In the three patients in which we performed frequency titrations (see Model Robustness Testing); we used the non-symptomatic, off-peak stimulations from those experiments as true negative stimulations.

Data availability

SPES data and all analysis algorithms will be provided on request by the corresponding author.

Results

SPES evoked responses are reconstructed with TFM

We first assessed whether the TFMs were able to accurately reconstruct the SPES evoked responses by calculating the fraction of data points that lay within 1 SD of the mean, calculated from all stimulation trials. We found that 97.7 ± 7.3% of the model-reconstructed

data points lay within 1 SD of the mean when assessed across all patients, indicating that our models were able to accurately capture the input–output behaviour of iEEG responses under SPES (Fig. 2A).[31,32] When stratified by individual patients, we found the lowest median concordance across all stimulation pairs in an individual patient was 96.2% (Fig. 2B).

Experimentally derived gains match model-derived gains

We next confirmed that the Bode plot output matched the neural physiology resulting from brain stimulation at various frequencies. Experimentally derived gains generally matched TFM-predicted gains represented by the Bode plots; the median (interquartile range) of the absolute value of the deviance of the experimentally derived gains from the Bode plot was 1.34 (interquartile range 0.54) when assessed across all patients (Fig. 3). We also plotted the experimental gains against the theoretical gains predicted by the Bode plot. In P027 and P031, the trajectories of the experimental gains closely followed the theoretical gains, with Pearson correlation coefficients of 0.99 and 0.88, respectively (Fig. 3A and B). In P032, the range of experimental gain values more closely matched the range of theoretical gains values in channels LABT5-6, but this was not true for LAI4-5 (Fig. 3C and D). It is worth noting that P032's SPES responses had strong artefacts that could not be entirely removed, probably leading to poorer TFMs and predictions.

Bode plot metrics distinguish surgical successes and failures

We tested whether the TFMs were able to localize the SOZ and anticipate surgical outcomes. We proposed that pathological resonance would be most prevalent in SOZ electrodes, thus we assessed whether our metric of resonance in the Bode plot, the PW ratio, was larger in SOZ nodes when compared to non-SOZ nodes in successful surgical outcomes. Further, we expected that the SOZ PW ratios would be less distinguishable from non-SOZ PW ratios in failed surgical outcomes. A representative example of a successful surgical outcome case is shown in the top panel of Fig. 4A, and a failed surgical outcome is shown in the bottom panel of Fig. 4A. SOZ regions have higher DC gains and higher peaks in the successful case. In the failure case, the SOZ region Bode plots are indistinguishable from the non-SOZ Bode plots, indicating an inability to differentiate seizure-generating tissue. The DC gain is the left-most point on the Bode plot and describes the magnitude of the output in response to a constant input.

We used a logistic regression model to distinguish successful versus failed outcomes with the PW ratio and other Bode plot features. We calculated the DC gain, the peak gain (max over all frequencies of the 2-norm of vector $\boldsymbol{H}$), the peak frequency (ω^*), the roll-off, the AUC (area) and the PW ratio (see Fig. 1C). We found that the inclusion of the PW ratio and the DC gain, modulated by whether the seizure onset was in neocortex or mesial temporal regions, best distinguished surgical outcomes (AUC of 0.83) (Fig. 4B). The probability value, $\hat{p}$, for surgical successes were significantly higher than those of surgical failures (Wilcoxon rank-sum test, $P = 0.008$) (Fig. 4C).

Bode plot metrics outperform CCEPs in seizure onset zone localization

In a similar way, we used a logistic regression model to distinguish successful and failed outcomes using metrics derived purely from CCEP amplitudes and spectral responses, which have been shown to localize SOZ regions.[25,26,33] We found that the best CCEP model included the *Z*-scores of the N2 amplitudes, and the *Z*-scores of the N1 amplitudes modulated by whether the seizure onset region was in neocortex or mesial temporal regions. The AUC for this curve was 0.76 and the $\hat{p}$ values were also statistically significantly different between successful and failed surgical outcomes (Wilcoxon rank-sum test, $P = 0.045$) (Fig. 4B and C). For CCSRs, the inclusion of the theta, alpha and beta frequency bands as features in the logistic regression model provided the greatest separation between surgical successes and failures, with an overall AUC of 0.70 (Fig. 4B). However, the $\hat{p}$ values were not statistically significantly greater in the patients with surgical success (Wilcoxon rank-sum test, $P = 0.07$) (Fig. 4C). Thus, our Bode features compared to and slightly outperformed current state-of-the-art SPES-derived metrics in distinguishing surgical outcomes (Fig. 4B). We note, however, that an additional advantage of the Bode plot features is that the frequency at which to induce seizures is predicted.

Bode model is robust to specific clinical factors

Studies have shown that the morphology or spectral content of evoked responses to SPES and cortical stimulation can depend on a variety of factors such as the recording electrode type,[34] the proximity to white matter,[35,36] the proximity to highly functional regions,[23,37,38] epilepsy type[39,40] and others. We tested whether the probability of success, as defined by the logistic regression model with Bode features, was significantly modulated by several of these factors.

The probability of success generated by the Bode model was significantly lower if the patient had a previous resection (Fig. 5A) (Wilcoxon rank-sum test $P = 0.037$); it was more likely that a patient would be seizure-free if they had not had a previous epilepsy surgery. The probability of success was not significantly correlated to whether the SOZ was mesial temporal or extratemporal onset (Fig. 5B), the recording electrode type (SEEG or ECoG) (Fig. 5C and Supplementary Fig. 3), a lesional or non-lesional MRI (Fig. 5D), the patient's age (Fig. 5E) or the patient's gender (Fig. 5F). Thus, although the SPES evoked waveform may differ due to these clinical and recording factors, our neural resonance metric remained robust to most of these factors in this small cohort of patients (Fig. 5).

Seizures induced by stimulating resonant nodes

We found that periodic stimulation of resonant nodes in the iEEG network elicited seizure activity or triggered seizures. Table 2 lists the retrospective patients in which seizures were induced by either SPES or functional mapping procedures and the prospective patients in which we tested whether seizures/auras could be elicited by stimulating predicted nodes at ω^*.

In 7 of the 11 patients, the periodic stimulating frequency that elicited the seizure, aura or after-discharges matched the Bode peak frequency, ω^* (Table 2). For example, P003 and P011 underwent functional mapping at 50 Hz as a presurgical work-up. The stimulation pairs that were tested were labelled within the SOZ, and stimulation of these sites induced the patient's native seizure. The Bode plots for each show a sharp peak at 50 Hz (Supplementary Fig. 4B and C). The two patients that did not have a matching Bode peak either elicited a non-native seizure (P025) or had a seizure onset region that was too broad for resection (P029) (Table 2).

On average, we stimulated 8.7 ± 3.7 pairs of electrodes at the resonant frequency, ω^*, to elicit seizures or trigger epileptogenic activity. In four of the six patients, prospectively stimulating at ω^* induced at least one seizure or aura, which we defined to be true

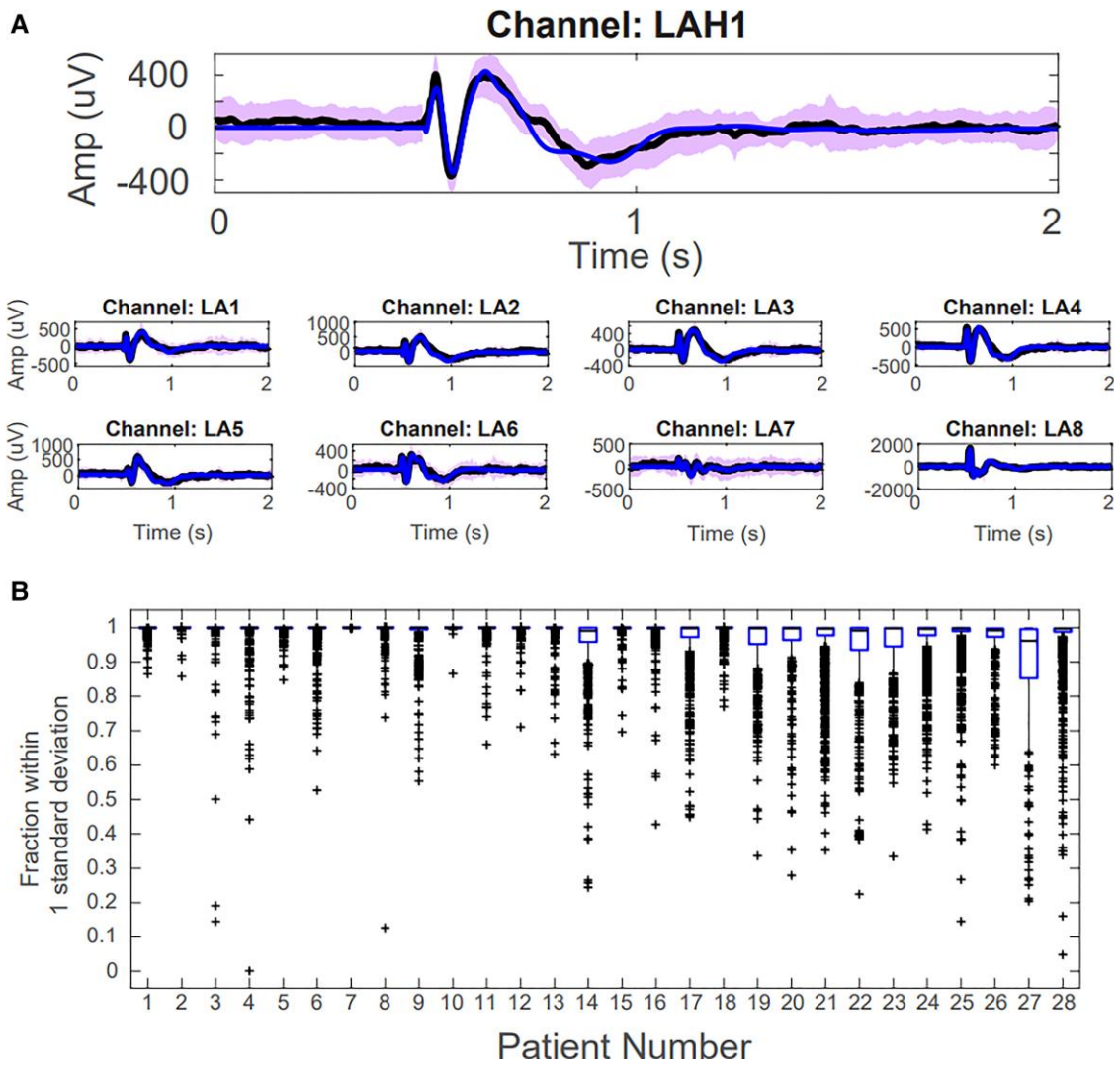

Figure 2 TFMs reconstruct the SPES evoked responses for representative response channels. (**A**) Representative examples of model reconstructions. The black line is the average evoked response from all trials, the blue line is the model reconstruction and the purple shaded area denotes 1 SD. (**B**) Box plots representing the fraction of data-points that lie within 1 SD of the mean for each channel and each stimulation pair, separated by patient.

positives (Fig. 6, Table 2, bottom). One caveat to this number is that when we built the TFMs for P032, there was substantial stimulation artefact remaining in the data and the model did not fit the data well. We prospectively stimulated based on this inaccurate model and seizures were elicited at two values of ω^*.

We defined true positives as a seizure or aura elicited at a resonant frequency, ω^*, predicted by the research team (Fig. 6A, C and E). For example, patient P028 underwent SPES and was investigated prospectively for seizures. One channel pair, LPH1-2, elicited an aura after 3 s of a 20 Hz stimulation period and another channel pair, RAH1-2, elicited a seizure after 3 s of an 18 Hz stimulation period (Fig. 6C). Sharp peaks in the Bode plots occur at these frequencies. Another true positive patient, Patient P031, was tested for SIS twice over 2 days (Fig. 6E). We performed the SPES procedure in the morning of the first day and tested for seizures in the afternoon. The frequency of stimulation was titrated from 1 Hz to the resonant frequency (13 Hz) in 1-Hz increments, and seizure was elicited at a 15 Hz stimulation frequency. The next day, we tested the same pair of electrodes and elicited another seizure at a 13-Hz stimulation frequency (Fig. 6E). Last, patient P024 was considered a true positive. This was the first patient we tested for prospectively stimulating SIS. Although the Bode plots suggested stimulating at 6 Hz (Fig. 6A), which is the resonant frequency, we stimulated at 20 Hz because previous literature indicated high frequencies may increase the chances of eliciting SIS.[14] We elicited two native auras in this patient, and it is unknown whether we would have triggered a seizure by stimulating at ω^*. However, we considered this case a true positive because stimulation channel LSM01 was not indicated as SOZ, early propagation or irritative zone, but stimulation of this area induced a native aura. This indicated that our resonance metric identified an epileptogenic region that may have remained hidden if only evaluated with current clinical practices (Fig. 6A).

In Table 2, the 'Number of Pairs Tested' indicates the number of tested resonant peaks that the clinical team, guided by the research team, prospectively stimulated at ω^*. The total number of false positives were the stimulations that only elicited after-discharges or no symptoms. In total, there were 47 false positive stimulations (Table 2, bottom).

There were three cases of false negatives. The clinical team stimulated seizures or auras based on their clinical hypotheses,

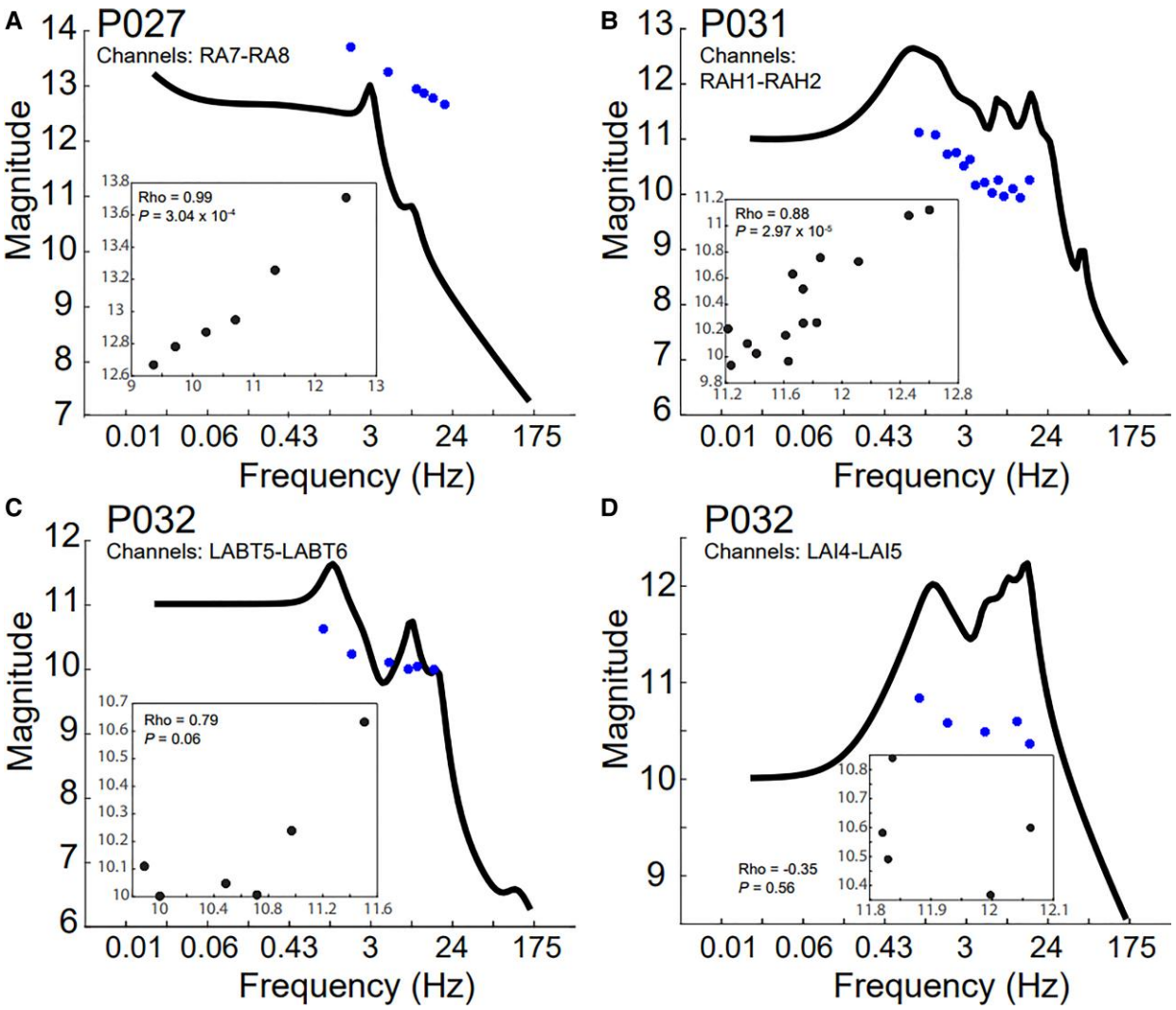

Figure 3 Experimentally derived gains match Bode plots. The system gains were experimentally calculated by computing the ratio of the Frobenius norm of the iEEG responses to the norm of the input pulse (blue circles) for (**A**) P027, (**B**) P031 and (**C** and **D**) P032. The experimentally derived gains were compared to the TFM-derived Bode plot (black line). The experimental gains (*y*-axis) were plotted against the theoretical gains (*x*-axis) along with the Pearson correlation coefficient and *P*-value associated with the comparison (*inset*).

but these stimulation parameters did not match a resonant peak in the corresponding Bode plot (Fig. 6B and D, Table 2, bottom). However, patient P030 was in the hospital for >2 weeks and had no spontaneous seizures captured. Therefore, it is unknown whether the seizure elicited in P030 was native to the patient (Fig. 6D). Additionally, although we did not prospectively list channel RHG1/3 to test, the frequency that elicited a seizure is not far away from the secondary resonant peak at 16 Hz (Fig. 6B).

Last, seizures or auras were only elicited in P031 while performing the frequency titrations used in the gain matching experiments (Fig. 3), thus we included the 26 off-peak stimulations as true negatives, the four on-peak stimulations that did not elicit seizures as false positives (included in the 47 total) and the one on-peak stimulation that elicited a seizure as a true positive.

Discussion

In this study, we investigated whether neural resonance, as measured by TFMs derived from SPES response data, could identify epileptogenic brain regions to target for stimulation to induce seizures in drug-resistant epilepsy patients. We first showed that pathologically resonant regions corresponded to seizure onset regions such that the presence or absence of resonance correlated with surgical outcomes. We further showed that our TFMs retrospectively and prospectively uncovered neural resonance by reflecting and predicting where and at what frequency epileptiform activity could be induced in four out of six patients.

Our novel resonance hypothesis is based on the presence of strong oscillators in the human brain.[41,42] In the well-studied visual cortex, electrophysiological experiments have shown that neurons synchronize their firing to the frequency of flickering light, leading to EEG responses that oscillate at the same frequency as the stimulus (steady-state visual evoked potentials).[43] Interestingly, it was shown that although the brain exhibits responses at all frequencies from 1 to 100 Hz, the oscillations evoked at specific frequencies were higher amplitude than what was expected by the 1/f nature of EEG oscillations.[44] This implied that the visual cortex exhibits resonance phenomena, i.e. the brain responds more strongly to some frequencies over others. Such a phenomenon is not unique to the visual cortex:

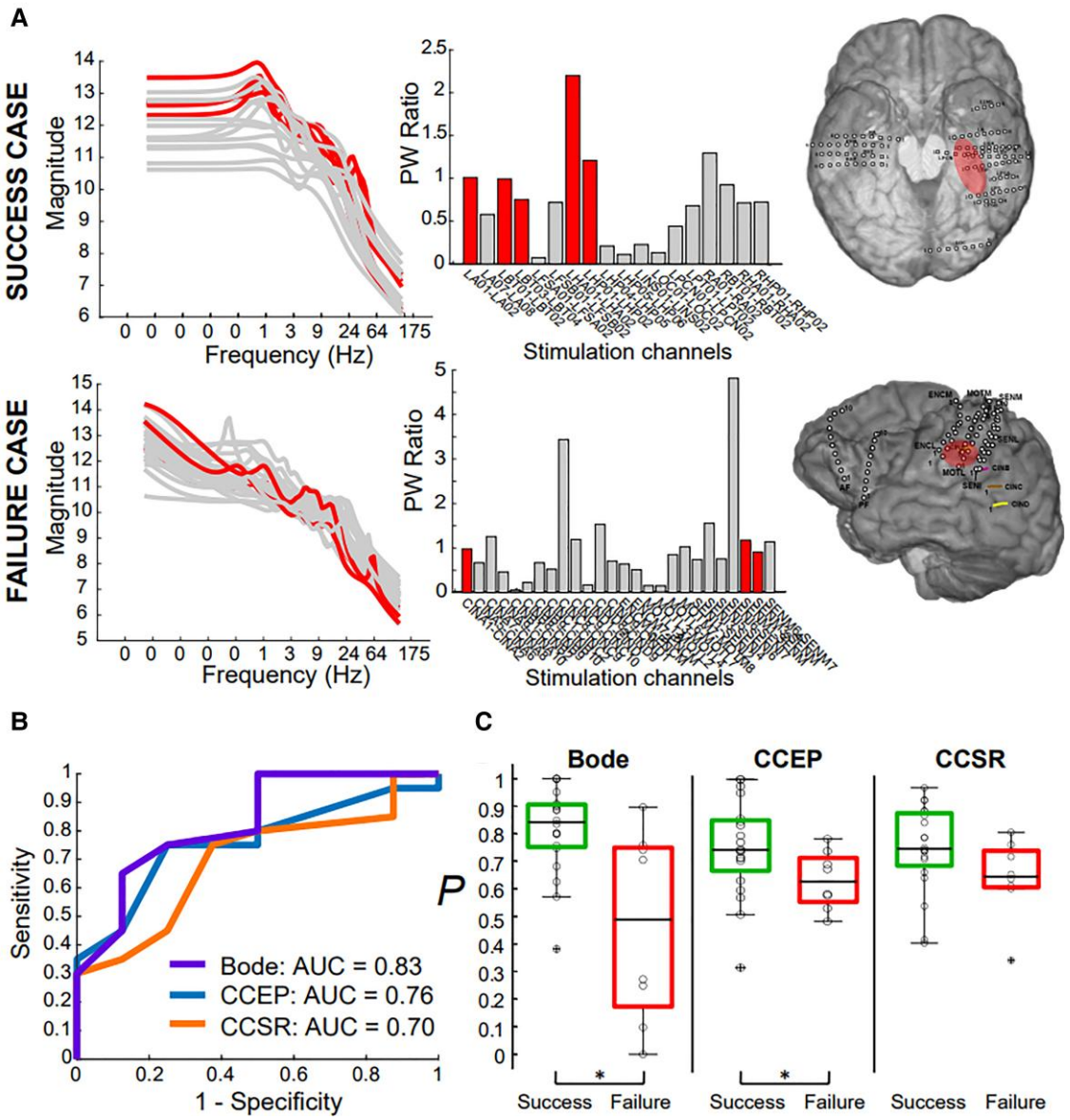

Figure 4 Bode plots and PW ratios reflect surgical outcome. (**A**) Representative patients with successful (P017, *top*) and failed (P011, *bottom*) surgical outcomes. The *left* and *middle* panels show the Bode plots and PW ratios for all stimulated channel pairs, respectively, and the *right* panel shows the SOZ location for both patients. (**B**) ROC analysis finds Bode features superior in discriminating successful and failed outcomes. Best Bode model included PW ratio and the DC gain as features with an AUC of 0.83; the best CCEP model included Z-scores from N2 and N1 amplitudes and had an AUC of 0.76; best CCSR model included theta, alpha and beta frequency bands with an AUC of 0.70. (**C**) The probability values for individual patients were significantly greater for surgical successes (green box plots, *left* box for each model) compared with failures (red box plots, *right* box for each model) in both Bode and CCEP models, but insignificantly greater in the CCSR model.

the alpha frequency range (8–12 Hz) also exhibits resonance during a variety of perceptual and cognitive functions from primary sensory coding to memory representations.[45,46] The resonance proposition has also been investigated computationally: in a model of the cortical column, one research study showed that neuronal tissue displays epileptic-like activity when exposed to enhanced stimulation of certain frequencies.[47]

We used data collected from patients that underwent SPES. In the past 10–15 years, SPES has become increasingly used as a tool to investigate functional and pathological connectivity in epilepsy and to localize epileptic networks.[24,25,33,48,49] SPES defines effective connections in the human brain because the neural evoked potentials are measured in direct response to the stimulation (Fig. 1B).[50] SPES has been used to map language[23] and motor networks,[37] as well as functional connections in a variety of brain structures.[51–57] In patients with epilepsy, it was found that the SPES evoked potentials, also known as CCEPs, were higher amplitude in the seizure onset and early spread regions when compared to healthy brain regions, indicating a decreased threshold of excitability.[25,26,39] It has also been reported that stimulation of epileptogenic regions trigger 'delayed responses', such as spikes or after-discharges, that occur 100 to 1 ms after stimulus onset.[24,48] Most importantly, it was shown that removal of areas that consistently exhibited these epileptiform features resulted in good outcomes, supporting the idea these evoked response biomarkers can be localizing for the SOZ.[24,58]

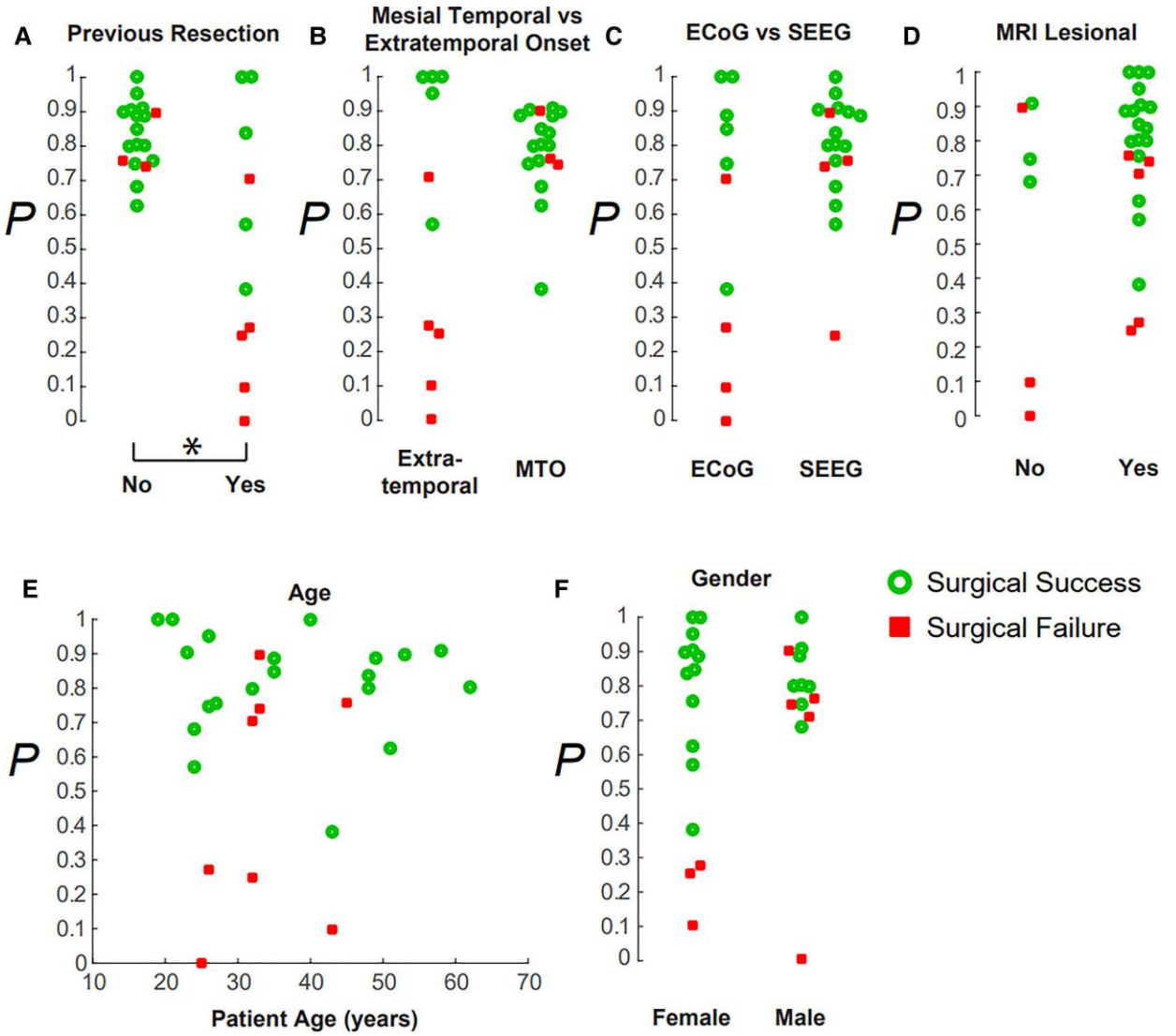

Figure 5 Bode models are robust to several clinical factors. The probability of success generated by the Bode model (**A**) was significantly higher if the patient had not had a previous resection. The probability of success was not significantly modulated by (**B**) a mesial temporal or extratemporal SOZ onset, (**C**) recording electrode type (ECoG or SEEG), (**D**) a lesional MRI, (**E**) patient age or (**F**) gender.

Although SPES responses have been shown to hold pertinent information about the epileptogenic network, the current clinical workflow does not include SPES for localization purposes. In fact, especially in the USA, electrical stimulation is almost solely used for functional mapping to define eloquent areas and not used in the definition of the epileptogenic network itself.[59] We posit that dynamical analysis of SPES data can provide novel insights into the epileptogenic network that may improve the efficacy of SIS for seizure onset localization.

We found that TFMs derived from the SPES data were physiologically relevant; the models closely predicted both iEEG responses to stimulation and output system gains. The Bode plots derived from the TFMs carried information that identified epileptogenicity, as revealed by the retrospective development logistic regression model. We found that a model constructed from two specific features of the Bode plot, the PW ratio and the DC gain, best distinguished surgical successes and failures. The DC gain was modulated by an indicator function, whether the clinically defined SOZ regions were in the mesial temporal structures or not. This distinction was derived from our previous work that showed that the mesial temporal structures have hub effects on the CCEP waveform, and this effect is accentuated if the mesial temporal region is epileptogenic.[33] Indeed, the PW ratios gleaned from stimulating mesial temporal regions were greater than stimulating in grey or white matter and significantly higher than stimulating regions that were outside these designations (Supplementary Fig. 5).

We benchmarked our resonance metric with state-of-the-art SPES algorithms that relied on the CCEP waveform or spectral signature. Currently, computational approaches that compute iEEG features on individual channels, such as the N1 or N2 peak amplitudes, latencies or spectral responses (Fig. 1B), often focus on waveform or power differences in individual channels to identify epileptogenic regions.[24,48] On the other hand, there are network-based computational approaches that compute static pairwise correlations and derive graph-theoretic measures from the adjacency matrices.[60] While these approaches can compute summary statistics of interest such as clustering coefficients and modularity and network hubs, such measures can have identical summary

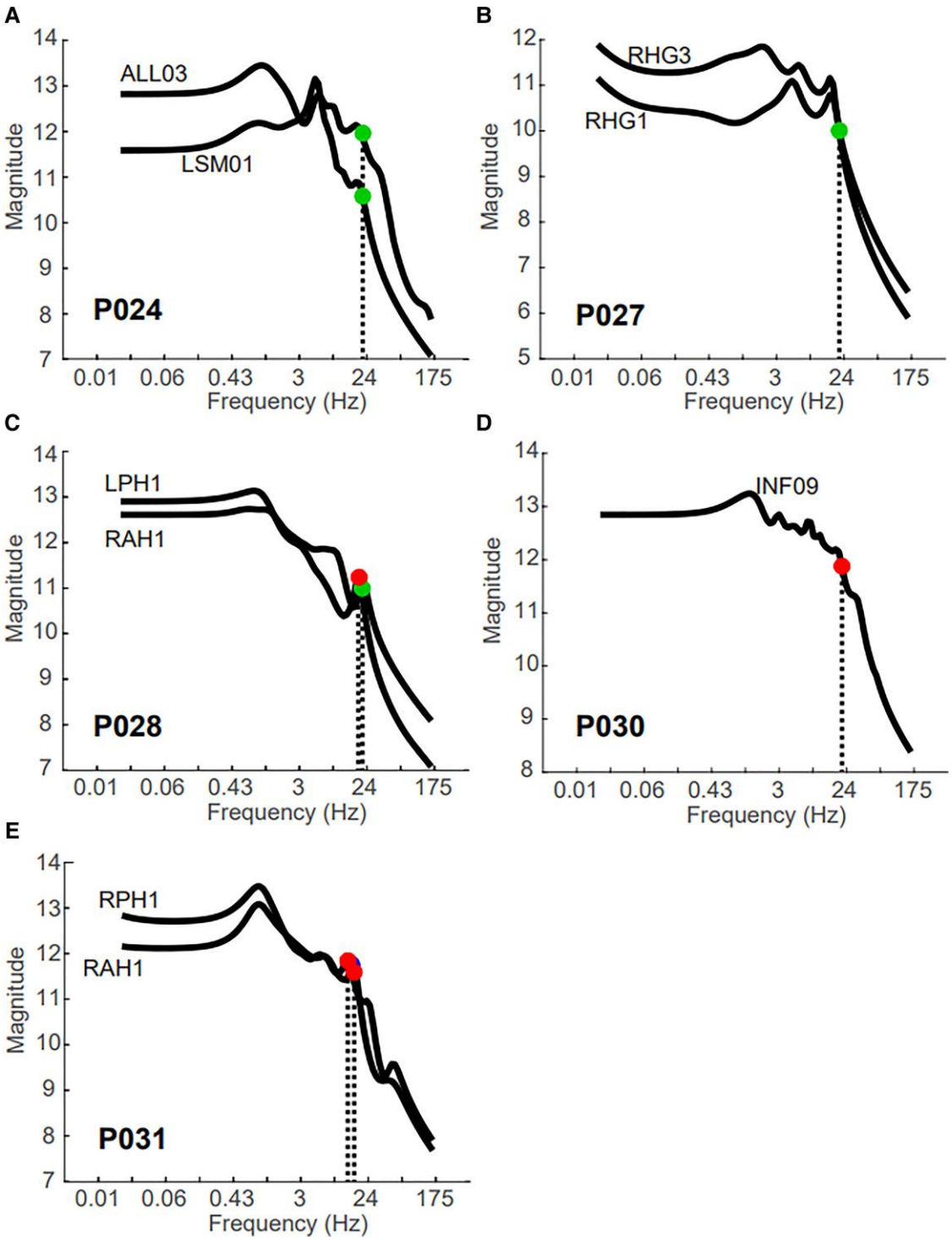

Figure 6 Seizures are prospectively stimulated in patients with corresponding resonant peaks in Bode plot. The black line shows the Bode plot for each stimulation pair and labelled with the first stimulation channel name for (**A**) P024, marked a true positive; (**B**) P027, marked a false negative; (**C**) P028, a true positive; (**D**) P030, a false negative and (**E**) P031, a true positive. The circles indicate the frequency of periodic stimulation that elicited a seizure (red) or aura (green).

statistics for drastically different networks. We found that our TFM-derived metrics was comparable to the CCEP and CCSR metrics in distinguishing to surgical outcomes (Bode AUC 0.83 versus CCEP AUC 0.76 versus CCSR AUC 0.70), but our metric provides resonant frequency information that the CCEP response alone cannot provide.

Our average rate of symptomatic stimulations (either seizure or aura) was 17% with all patients combined, which is comparable to earlier investigations of SIS.[14] Additionally, because we tested electrodes that were least likely to produce seizures (not in the hypothesized SOZ) to most likely (within the hypothesized SOZ), the seizure induction rate may have been higher if we chose to

stimulate the most suspect nodes first. We also found that higher stimulation frequencies (>10 Hz) exhibited a higher likelihood of eliciting seizures, corroborating previous studies.[30,61]

There were some instances where the resonant peaks of our Bode plots did not align with the frequency used to stimulate the seizures (Supplementary Fig. 4). Interestingly, out of the five retrospective patients with surgical outcomes, the two patients that did not have resonant peaks in the stimulated areas (i) had seizure onset regions that were too broad for resection (P029); or (ii) stimulated a non-native seizure in the patient (P025). This possibly indicates that core SOZ nodes possess more resonant properties than fringe nodes, or there was possibly an under sampling of the true epileptogenic zone.

The robustness of our algorithm to temporal and brain state changes must be determined in a future study. For example, if the Bode plots show resonant peaks when SPES was performed, will that region be resonant at the same frequency the next day? In our study, patients were stimulated for seizures ~1 h after completing the SPES procedure for the subset of electrode pairs. However, in patient P031, we performed the SPES procedure in the morning and tested for seizures both in the afternoon and the following day. We were able to specifically elicit a seizure at or close to the resonant frequency over 24 h apart (Fig. 6A). This example suggests a robustness of these resonant regions and frequencies across time, but a larger validation study will be required to examine this directly. Future work is also warranted to determine the range of frequencies around a peak frequency that may also trigger a seizure. For example, stimulation of specific regions with large resonant peaks in patient P024 triggered native auras, but the frequency was not at the peak frequency, ω^*. It is unknown whether a stronger response, i.e. a seizure, could have been elicited if ω^* had been stimulated. The sensitivity of the brain to slightly off-peak frequencies will be a subject of future study.

Another question that emerges from this study is whether this type of resonance also occurs in healthy brain tissue. If so, it is possible that our resonance algorithm may identify resonant regions regardless of whether these regions are in pathological brain tissue. It can be hypothesized that if a resonant brain region is stimulated and it does not induce the patient's native seizure, perhaps that region is not part of the SOZ. Whereas, if a resonant region that was not originally included in the SOZ triggers a seizure that looks similar to the native seizure, perhaps it can be concluded that this region may bring seizure freedom if removed. For example, patient P030 had no spontaneous seizures before we elicited a seizure by stimulating contacts INF09-10. Thus, we cannot determine whether or not this seizure was native to the patient beyond anecdotal semiology from the family. A prospective study that evaluates outcome on the basis of stimulated seizures that were predicted from the TFMs will be necessary to investigate whether physiological resonance may interfere with our algorithm. A spatial map of physiological peak resonant frequencies across different brain regions would aid in identifying pathologically resonant regions, but a larger prospective study will be needed to answer this question. Additionally, a next step is to investigate whether the resonant frequencies identified in the Bode plots are present in the patient's seizure dynamics. If the Bode plot presents a strong peak at 10 Hz, is there a strong accompanying spectral signature at 10 Hz in the patient's ictal iEEG? We believe this could help characterize the spectral dynamics of the underlying network on a patient-specific basis.

This work may also translate to other fields of neuroengineering. We speculate that Bode plots could not only guide clinicians in what frequency to stimulate to elicit a seizure, it would also provide which frequencies to avoid when programming stimulating devices for seizure control. Also, given that certain stimulation frequencies can inhibit neuronal activity in certain areas such as with Parkinson's cases,[62] we may hypothesize that this phenomenon could be due to stimulation at off-peak frequencies.

This study pioneers the use of TFMs of SPES responses to identify resonant regions in the human brain that can be targeted to induce SIS to localize epileptogenic regions. TFMs are part of a unique branch of dynamical models that capture how nodes in a network dynamically interact with each other, and can be used to uncover internal properties of the underlying system including bandwidth, stability, controllability and system gain.[63–65] We showed that TFMs can be used to reveal resonant regions of the patient's epileptogenic network without the need to capture seizures beforehand. Currently, in the USA, the practice of stimulating to induce seizures is not often used due to uncertainty that the stimulated seizure is the patient's native seizure.[14,30,66] Additionally, even if the clinical team wants to perform stimulation to elicit a seizure as part of the SOZ localization investigation, there are no current methods that guide where or at what frequency to stimulate. To address these issues, these results indicate that SPES-derived TFMs can reveal resonant nodes, identify resonant frequencies at which to stimulate, and elicit the patient's native seizure. Incorporation of these methods into the clinical workflow would remove the need to passively wait on the patient's seizures to occur naturally.

The identification of the SOZ is a manual, team-based process that seeks to synthesize large amounts of disparate neural data. Although there are software tools that indicate when a seizure has occurred, there are currently no FDA-approved software tools used in the clinical workflow that identify where the seizures occur.[67] In this work, we have proposed a biomarker of neural resonance that can guide clinicians in eliciting native seizures to localize seizure onset regions. We believe incorporation of these computational methods into current clinical practice will improve the current gold standard in intracranial monitoring for SOZ localization by reducing the length of stay for patients and improving their chances of seizure freedom after surgery.

Acknowledgements

The authors would like to acknowledge the EEG technicians at the JHH EMU for their exemplary patient care.

Funding

R.J.S. was funded by an NIH IRACDA Fellowship through the ASPIRE program at Johns Hopkins University. S.V.S. was supported by R01 NS125897.

Competing interests

The authors report no competing interests.

Supplementary material

Supplementary material is available at *Brain* online.

References

1. Cardarelli WJ, Smith BJ. The burden of epilepsy to patients and payers. *Am J Manag Care*. 2010;16:S331–S336.

2. Granata T, Marchi N, Carlton E, *et al*. Management of the patient with medically refractory epilepsy. *Expert Rev Neurother*. 2009;9: 1791–1802.
3. Lüders HO, Najm I, Nair D, Widdess-Walsh P, Bingman W. The epileptogenic zone: general principles. *Epileptic Disord*. 2006; 8: 1–9.
4. Jobst BC, Cascino GD. Resective epilepsy surgery for drug-resistant focal epilepsy: A review. *JAMA*. 2015;313:285–293.
5. Malmgren K, Edelvik A. Long-term outcomes of surgical treatment for epilepsy in adults with regard to seizures, antiepileptic drug treatment and employment. *Seizure*. 2017;44:217–224.
6. González-Martínez JA, Srikijvilaikul T, Nair D, Bingaman WE. Long-term seizure outcome in reoperation after failure of epilepsy surgery. *Neurosurgery*. 2007;60:873–879.
7. Bulacio JC, Jehi L, Wong C, *et al*. Long-term seizure outcome after resective surgery in patients evaluated with intracranial electrodes. *Epilepsia*. 2012;53:1722–1730.
8. McIntosh AM, Kalnins RM, Mitchell LA, Fabinyi GCA, Briellmann RS, Berkovic SF. Temporal lobectomy: Long-term seizure outcome, late recurrence and risks for seizure recurrence. *Brain*. 2004;127:2018–2030.
9. Panigrahi M, Jayalakshmi S. Presurgical evaluation of epilepsy. *J Pediatr Neurosci*. 2008;3:74–81.
10. Begley CE, Durgin TL. The direct cost of epilepsy in the United States: A systematic review of estimates. *Epilepsia*. 2015;56: 1376–1387.
11. Kovács S, Tóth M, Janszky J, *et al*. Cost-effectiveness analysis of invasive EEG monitoring in drug-resistant epilepsy. *Epilepsy Behav*. 2021;114:107488.
12. Kämpfer C, Racz A, Quesada CM, Elger CE, Surges R. Predictive value of electrically induced seizures for postsurgical seizure outcome. *Clin Neurophysiol*. 2020;131:2289–2297.
13. Oderiz CC, Von Ellenrieder N, Dubeau F, *et al*. Association of cortical stimulation-induced seizure with surgical outcome in patients with focal drug-resistant epilepsy. *JAMA Neurol*. 2019;76: 1070–1078.
14. Kovac S, Kahane P, Diehl B. Seizures induced by direct electrical cortical stimulation – mechanisms and clinical considerations. *Clin Neurophysiol*. 2016;127:31–39.
15. Munari C, Kahane P, Tassi L, *et al*. Intracerebral low frequency electrical stimulation: A new tool for the definition of the "epileptogenic area"? *Adv Stereotact Funct Neurosurg*. 1993;58:181–185.
16. Kahane P, Tassi L, Francione S, Hoffmann D, Lo Russo G, Munari C. Manifestations électrocliniques induites par la stimulation électrique intracérébrale par «chocs dans les épilepsies temporales. *Neurophysiol Clin/Clin Neurophysiol*. 1993;23:305–326.
17. Quirk JA, Fish DR, Smith SJM, Sander JWAS, Shorvon SD, Allen PJ. Incidence of photosensitive epilepsy: A prospective national study. *Electroencephalogr Clin Neurophysiol*. 1995;95:260–267.
18. Padmanaban V, Inati S, Ksendzovsky A, Zaghloul K. Clinical advances in photosensitive epilepsy. *Brain Res*. 2019;1703:18–25.
19. Faingold C, Tupal S, N'Gouemo P. *Genetic Models of Reflex Epilepsy and SUDEP in Rats and Mice*. In: Pitkänen A, Buckmaster PS, Galanopoulou AS, Moshe S, eds. *Models of Seizures and Epilepsy*. 2nd Ed. Elsevier Inc; 2017:441–453.
20. Kesner RP. Subcortical mechanisms of audiogenic seizures. *Exp Neurol*. 1966;15:192–205.
21. Li A, Inati S, Zaghloul K, Sarma S. Fragility in epileptic networks: The epileptogenic zone. In: *Proceedings of the American Control Conference*. AACC. 2017:2817–2822. doi:10.23919/ACC.2017.7963378
22. D'Aleo R, Rouse A, Schieber M, Sarma SV. Quantifying Interactions between Neural Populations during Behavior using Dynamical Systems Models. In: *Proceedings of the Annual International Conference of the IEEE Engineering in Medicine and Biology Society, EMBS*. IEEE. 2019:1960–1964. doi:10.1109/EMBC.2019.8856678
23. Matsumoto R, Nair DR, LaPresto E, *et al*. Functional connectivity in the human language system: A cortico-cortical evoked potential study. *Brain*. 2004;127:2316–2330.
24. Valentín A, Alarcón G, García-Seoane JJ, *et al*. Single-pulse electrical stimulation identifies epileptogenic frontal cortex in the human brain. *Neurology*. 2005;65:426–435.
25. Iwasaki M, Enatsu R, Matsumoto R, *et al*. Accentuated cortico-cortical evoked potentials in neocortical epilepsy in areas of ictal onset. *Epileptic Disord*. 2010;12:292–302.
26. Enatsu R, Piao Z, O'Connor T, *et al*. Cortical excitability varies upon ictal onset patterns in neocortical epilepsy: A cortico-cortical evoked potential study. *Clin Neurophysiol*. 2012;123:252–260.
27. Gkogkidis CA, Wang X, Schubert T, *et al*. Closed-loop interaction with the cerebral cortex using a novel micro-ECoG-based implant: The impact of beta vs. Gamma stimulation frequencies on cortico-cortical spectral responses*. *Brain-Computer Interfaces*. 2017;4:214–224.
28. Mitsuhashi T, Sonoda M, Iwaki H, Luat AF, Sood S, Asano E. Effects of depth electrode montage and single-pulse electrical stimulation sites on neuronal responses and effective connectivity. *Clin Neurophysiol*. 2020;131:2781–2792.
29. Mostame P, Sadaghiani S. Oscillation-based connectivity architecture is dominated by an intrinsic spatial organization, not cognitive state or frequency. *J Neurosci*. 2021;41:179–192.
30. Trebuchon A, Racila R, Cardinale F, *et al*. Electrical stimulation for seizure induction during SEEG exploration: A useful predictor of postoperative seizure recurrence? *J Neurol Neurosurg Psychiatry*. 2021;92:22–26.
31. Kamali G, Smith RJ, Hays M, *et al*. Transfer function models for the localization of seizure onset zone from cortico-cortical evoked potentials. *Front Neurol*. 2020;11:579961.
32. Smith RJ, Kamali G, Hays M, *et al*. State-space models of evoked potentials to localize the seizure onset zone. In: *Proceedings of the Annual International Conference of the IEEE Engineering in Medicine and Biology Society, EMBS*. Montreal, Canada. 2020:2528–2531. doi:10.1109/EMBC44109.2020.9176697
33. Hays MA, Coogan C, Crone NE, Kang JY. Graph theoretical analysis of evoked potentials shows network influence of epileptogenic mesial temporal region. *Hum Brain Mapp*. 2021;42:4173–4186.
34. Prime D, Rowlands D, O'Keefe S, Dionisio S. Considerations in performing and analyzing the responses of cortico-cortical evoked potentials in stereo-EEG. *Epilepsia*. 2018;59:16–26.
35. Kundu B, Davis TS, Philip B, *et al*. A systematic exploration of parameters affecting evoked intracranial potentials in patients with epilepsy. *Brain Stimul*. 2020;13:1232–1244.
36. Mohan UR, Watrous AJ, Miller JF, *et al*. The effects of direct brain stimulation in humans depend on frequency, amplitude, and white-matter proximity. *Brain Stimul*. 2020;13:1183–1195.
37. Matsumoto R, Nair DR, LaPresto E, Bingaman W, Shibasaki H, Lüders HO. Functional connectivity in human cortical motor system: A cortico-cortical evoked potential study. *Brain*. 2007;130:181–197.
38. Basu I, Robertson MM, Crocker B, *et al*. Consistent linear and non-linear responses to invasive electrical brain stimulation across individuals and primate species with implanted electrodes. *Brain Stimul*. 2019;12:877–892.
39. Hays MA, Smith RJ, Haridas B, Coogan C, Crone NE, Kang JY. Effects of stimulation intensity on intracranial cortico-cortical evoked potentials: A titration study. *Clin Neurophysiol*. 2021; 132:2766–2777.
40. Guo Z-H, Zhao B-T, Toprani S, *et al*. Epileptogenic network of focal epilepsies mapped with cortico-cortical evoked potentials. *Clin Neurophysiol*. 2020;131:2657–2666.

41. Kalamangalam G, Slater JD. Periodic lateralized epileptiform discharges and after discharges: Common dynamic mechanisms. *J Clin Neurophysiol*. 2016;32:331–340.
42. Kuramoto Y. Self-entrainment of a population of coupled nonlinear oscillators. In: International Symposium on Mathematical Problems in Theoretical Physics. 1975:420–422.
43. Vialatte FB, Maurice M, Dauwels J, Cichocki A. Steady-state visually evoked potentials: Focus on essential paradigms and future perspectives. *Prog Neurobiol*. 2010;90:418–438.
44. Herrmann CS. Human EEG responses to 1–100 Hz flicker: Resonance phenomena in visual cortex and their potential correlation to cognitive phenomena. *Exp Brain Res*. 2001;137:346–353.
45. Başar E. A review of alpha activity in integrative brain function: Fundamental physiology, sensory coding, cognition and pathology. *Int J Psychophysiol*. 2012;86:1–24.
46. Başar E, Başar-Eroglu C, Karakaş S, Schürmann M. Brain oscillations in perception and memory. *Int J Psychophysiol*. 2000;35:95–124.
47. Jedynak M, Pons AJ, Garcia-Ojalvo J, Goodfellow M. Temporally correlated fluctuations drive epileptiform dynamics. *Neuroimage*. 2017;146:188–196.
48. Valentin A, Anderson M, Alarcón G, *et al*. Responses to single pulse electrical stimulation identify epileptogenesis in the human brain in vivo. *Brain*. 2002;125:1709–1718.
49. Matsumoto R, Kunieda T, Nair D. Single pulse electrical stimulation to probe functional and pathological connectivity in epilepsy. *Seizure*. 2017;44:27–36.
50. Keller CJ, Honey CJ, Mégevand P, Entz L, Ulbert I, Mehta AD. Mapping human brain networks with cortico-ortical evoked potentials. *Philos Trans R Soc B Biol Sci*. 2014;369:20130528.
51. Lacruz ME, García Seoane JJ, Valentin A, Selway R, Alarcón G. Frontal and temporal functional connections of the living human brain. *Eur J Neurosci*. 2007;26:1357–1370.
52. Matsumoto R, Nair DR, Ikeda A, *et al*. Parieto-frontal network in humans studied by cortico-cortical evoked potential. *Hum Brain Mapp*. 2012;33:2856–2872.
53. Enatsu R, Gonzalez-Martinez J, Bulacio J, *et al*. Connections of the limbic network: A corticocortical evoked potentials study. *Cortex*. 2015;62:20–33.
54. Almashaikhi T, Rheims S, Jung J, *et al*. Functional connectivity of insular efferences. *Hum Brain Mapp*. 2014;35:5279–5294.
55. Dionisio S, Mayoglou L, Cho SM, *et al*. Connectivity of the human insula: A cortico-cortical evoked potential (CCEP) study. *Cortex*. 2019;120:419–442.
56. Kubota Y, Enatsu R, Gonzalez-Martinez J, *et al*. In vivo human hippocampal cingulate connectivity: A corticocortical evoked potentials (CCEPs) study. *Clin Neurophysiol*. 2013;124:1547–1556.
57. Mégevand P, Groppe DM, Bickel S, *et al*. The hippocampus and amygdala are integrators of neocortical influence: A corticocortical evoked potential study. *Brain Connect*. 2017;7:648–660.
58. Flanagan D, Valentín A, García Seoane JJ, Alarcón G, Boyd SG. Single-pulse electrical stimulation helps to identify epileptogenic cortex in children. *Epilepsia*. 2009;50:1793–1803.
59. Corley JA, Nazari P, Rossi VJ, *et al*. Cortical stimulation parameters for functional mapping. *Seizure*. 2017;45:36–41.
60. Zhao C, Liang Y, Li C, *et al*. Localization of epileptogenic zone based on cortico-cortical evoked potential (CCEP): A feature extraction and graph theory approach. *Front Neuroinform*. 2019;13:1–9.
61. Zangaladze A, Sharan A, Evans J, *et al*. The effectiveness of low-frequency stimulation for mapping cortical function. *Epilepsia*. 2008;49:481–487.
62. Dostrovsky JO, Levy R, Wu JP, Hutchison WD, Tasker RR, Lozano AM. Microstimulation-induced inhibition of neuronal firing in human globus pallidus. *J Neurophysiol*. 2000;84:570–574.
63. Ogata K. *Modern control engineering*. 5th ed. Prentice Hall; 2010.
64. Li A, Huynh C, Fitzgerald Z, *et al*. Neural fragility as an EEG marker of the seizure onset zone. *Nat Neurosci*. 2021;24:1465–1474.
65. Gunnarsdottir KM, Li A, Smith RJ, *et al*. Source-sink connectivity: A novel resting-state EEG marker of the epileptogenic zone. *bioRxiv*. [Preprint] https://doi.org/10.1101/2021.10.15.464594
66. Bernier GP, Richer F, Giard N, *et al*. Electrical stimulation of the human brain in epilepsy. *Epilepsia*. 1990;31:513–520.
67. Scheuer ML, Bagic A, Wilson SB. Spike detection: Inter-reader agreement and a statistical Turing test on a large data set. *Clin Neurophysiol*. 2017;128:243–250.